Distinct synthetic Aβ prion strains producing different amyloid deposits in bigenic mice

Jan Stöhr[a,b], Carlo Condello[a], Joel C. Watts[a,b,1], Lillian Bloch[a], Abby Oehler[c], Mimi Nick[d], Stephen J. DeArmond[a,c], Kurt Giles[a,b], William F. DeGrado[d], and Stanley B. Prusiner[a,b,2]

[a]Institute for Neurodegenerative Diseases, Departments of [b]Neurology and [c]Pathology, and [d]Pharmaceutical Chemistry, University of California, San Francisco, CA 94143

Contributed by Stanley B. Prusiner, May 14, 2014 (sent for review April 15, 2014)

An increasing number of studies continue to show that the amyloid β (Aβ) peptide adopts an alternative conformation and acquires transmissibility; hence, it becomes a prion. Here, we report on the attributes of two strains of Aβ prions formed from synthetic Aβ peptides composed of either 40 or 42 residues. Modifying the conditions for Aβ polymerization increased both the protease resistance and prion infectivity compared with an earlier study. Approximately 150 d after intracerebral inoculation, both synthetic Aβ40 and Aβ42 prions produced a sustained rise in the bioluminescence imaging signal in the brains of bigenic Tg(APP23:*Gfap*-luc) mice, indicative of astrocytic gliosis. Pathological investigations showed that synthetic Aβ40 prions produced amyloid plaques containing both Aβ40 and Aβ42 in the brains of inoculated bigenic mice, whereas synthetic Aβ42 prions stimulated the formation of smaller, more numerous plaques composed predominantly of Aβ42. Synthetic Aβ40 preparations consisted of long straight fibrils; in contrast, the Aβ42 fibrils were much shorter. Addition of 3.47 mM (0.1%) SDS to the polymerization reaction produced Aβ42 fibrils that were indistinguishable from Aβ40 fibrils produced in the absence or presence of SDS. Moreover, the Aβ amyloid plaques in the brains of bigenic mice inoculated with Aβ42 prions prepared in the presence of SDS were similar to those found in mice that received Aβ40 prions. From these results, we conclude that the composition of Aβ plaques depends on the conformation of the inoculated Aβ polymers, and thus, these inocula represent distinct synthetic Aβ prion strains.

Alzheimer's disease | in vitro | neurodegenerative diseases

Alzheimer's disease (AD) is a slowly progressive dementia characterized by the extracellular deposition of amyloid β (Aβ) peptide and the intraneuronal accumulation of neurofibrillary tangles composed of tau. Although most AD cases are sporadic, some are caused by mutations in the APP gene or components of the γ-secretase enzyme complex (1). To explain the late onset of heritable AD, one of us (S.B.P.) proposed that a second event must occur, which is the sustained accumulation of Aβ prions (2). Notably, mutations in the tau gene do not cause AD; rather, they are responsible for some familial forms of the frontotemporal dementias (3).

With the discovery that both kuru and Creutzfeldt-Jakob disease (CJD) are transmissible to apes and monkeys, Goudsmit et al. attempted to transmit AD to monkeys. Initially, they reported that two cases of familial AD (fAD) transmitted a CJD-like disease to monkeys, but this was not repeatable (4). These negative findings created a dichotomy in the minds of many investigators who assumed that AD, in contrast to CJD, could not be transmitted experimentally.

The inoculation of marmosets with brain homogenates from sporadic AD, fAD, or Down syndrome cases provided the first evidence for the transmissibility of AD (5). The recipient animals developed Aβ amyloid deposits in their brains, but control-inoculated primates did not. An experimental system in rodents for measuring Aβ prions was developed using Tg(APP23) mice that express the human APP gene carrying the Swedish mutation (6). This mutation encodes the substitution of two amino acids in APP that results in elevated levels of WT Aβ peptides in the brains of both patients and Tg(APP23) mice (7, 8). Both intracerebral and i.p. inoculation of Tg(APP23) mice accelerated the deposition of Aβ aggregates, many of which coalesced into amyloid plaques (9). To monitor Aβ prion replication in vivo, we used bioluminescence imaging (BLI) to measure the up-regulation of glial fibrillary acidic protein (GFAP) (10). To test whether Aβ or an unknown molecule in our purified preparations caused the BLI signal to increase, we polymerized synthetic Aβ40 into amyloid and injected the samples intracerebrally into Tg(APP23:*Gfap*-luc) mice (11). At ∼220 d postinoculation (dpi), the mice exhibited an increase in the BLI signal that correlated with widespread amyloid deposition, arguing that Aβ40 peptides in a prion conformation are sufficient to stimulate nascent Aβ amyloid deposition.

Because Aβ42 is more neurotoxic and amyloidogenic than Aβ40, we investigated the differences in transmissibility of the two peptides. Using a modified protocol, we polymerized both synthetic Aβ40 and Aβ42 into amyloids and inoculated the polymeric preparations intracerebrally into Tg(APP23:*Gfap*-luc) mice. We report here that Aβ42 amyloid preparations exhibited structural differences and produced neuropathological changes that are distinct from those of Aβ40. Although the Aβ40 prions produced cerebral deposits composed of both Aβ40 and Aβ42 amyloid, Aβ42 prions induced small plaques containing predominantly Aβ42. SDS perturbed the polymerization of Aβ42, resulting in amyloid that was indistinguishable ultrastructurally from Aβ40. Inoculation of the Aβ42 prions prepared with SDS resulted in the deposition of large amyloid plaques containing

NEUROSCIENCE

Significance

Alzheimer's disease is the most common neurodegenerative disorder; it is a progressive dementia for which there is currently no effective therapeutic intervention. The brains of patients with Alzheimer's disease exhibit numerous amyloid β (Aβ) amyloid plaques and tau-laden neurofibrillary tangles. Our studies show that synthetic Aβ peptides can form prions that infect mice and induce Aβ amyloid plaque pathology. Two different Aβ prion strains were produced from Aβ peptides. When injected into transgenic mice, one Aβ strain produced large plaques and the other strain induced small but more numerous plaques. Our findings may help to delineate the molecular pathogenesis of Alzheimer's disease and the development of anti-Aβ prion therapeutics.

Author contributions: J.S., C.C., and S.B.P. designed research; J.S., C.C., J.C.W., L.B., A.O., and M.N. performed research; J.S., C.C., S.J.D., K.G., W.F.D., and S.B.P. analyzed data; and J.S. and S.B.P. wrote the paper.

The authors declare no conflict of interest.

[1]Present address: Tanz Centre for Research in Neurodegenerative Diseases, University of Toronto, Toronto, ON, Canada.

[2]To whom correspondence should be addressed. E-mail: stanley@ind.ucsf.edu.

This article contains supporting information online at www.pnas.org/lookup/suppl/doi:10.1073/pnas.1408968111/-/DCSupplemental.

Downloaded at Palestinian Territory, occupied on December 16, 2021

www.manaraa.com

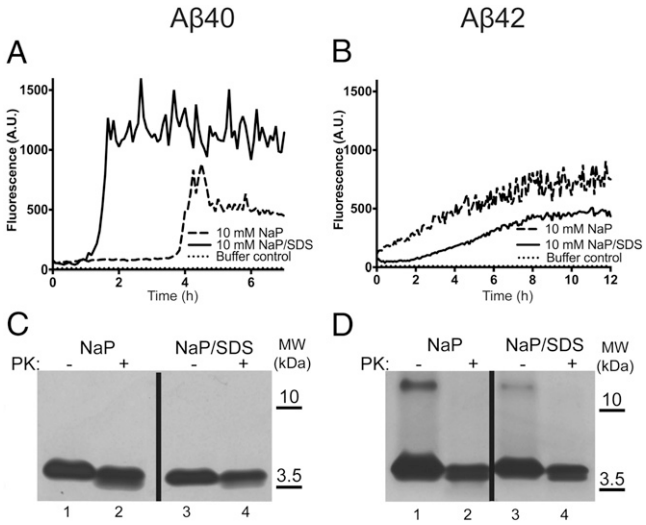

Fig. 1. Formation of synthetic Aβ40 (*A* and *C*) and Aβ42 (*B* and *D*) prions. (*A* and *B*) Kinetics of amyloid formation of Aβ40 (*A*) and Aβ42 (*B*) in NaP (dashed line) or NaP/SDS (solid line) buffer at 37 °C under constant agitation. The reaction with buffer alone (dotted line) is shown as a control. Fibril formation was measured by the increase in ThT (10 μM) fluorescence. (*C* and *D*) Silver-stained SDS/PAGE of the Aβ40 (*C*) or Aβ42 (*D*) amyloids revealed PK-resistant fractions (Aβ concentration, 0.2 mg/mL; PK concentration, 0.05 mg/mL). Molecular weight markers of migrated protein standards are shown in kilodaltons.

both Aβ40 and Aβ42 that were similar to those induced by Aβ40 prions.

Results

Having found that synthetic Aβ peptides could be folded into a conformation that became self-propagating (11), we asked if altering the folding conditions might increase the specific infectivity of our preparations. We began by dispersing the lyophilized Aβ40 and Aβ42 peptides in hexafluoroisopropanol that has been widely used to denature Aβ peptides before resuspension in DMSO and subsequent dilution in aqueous buffers (12). We chose two different conditions for the formation of amyloids fibrils from synthetic Aβ40 and Aβ42: the first consisted of 10 mM sodium phosphate (NaP) buffer at neutral pH (7.4) and the second was 10 mM NaP with the addition of 3.47 mM [0.1% (wt/vol)] SDS. This lower concentration of SDS was chosen because 8.67 mM [0.25% (wt/vol)] SDS prevented amyloid fibril formation as monitored by Thioflavin T (ThT) fluorescence (Fig. S1).

Aβ40 amyloid fibrils formed in the NaP buffer after a lag phase of ∼4 h (Fig. 1*A*, dashed line), whereas addition of 0.1% SDS shortened the lag phase to ∼1 h (solid line). In contrast, when Aβ42 amyloid fibrils were formed without SDS, a lag phase was virtually absent (Fig. 1*B*, dashed line), whereas addition of SDS resulted in a lag phase of ∼2 h (solid line). After the Aβ amyloids were formed, the samples were centrifuged at 100,000 × *g* for 1 h at 4 °C, the supernatant was discarded, and the pellet was resuspended in PBS and used for the studies described below.

Each of the amyloidogenic Aβ samples was assayed for resistance to limited proteolysis by measuring the amount of Aβ (200 μg/mL) remaining in the sample after incubation with proteinase K (PK; 50 μg/mL) for 1 h at 37 °C. As shown by silver-stained SDS/PAGE, the majority of both Aβ40 and Aβ42 in the presence or absence of 0.1% SDS resisted degradation (Fig. 1 *C* and *D*).

Following biochemical characterization, polymerized Aβ samples were also examined by transmission electron microscopy (TEM) (Fig. 2 and Fig. S2). In samples composed of Aβ40 that were polymerized in NaP buffer, numerous straight fibrils were observed after negative staining with 2% (wt/vol) ammonium molybdate (Fig. 2*A*). For Aβ42, we found both long straight fibrils and numerous short ones of <100 nm in length (Fig. 2*B*), which were scarce in the Aβ40 preparations. Addition of 0.1% SDS did not dramatically alter the appearance of the Aβ40 fibrils (Fig. 2*C*) but profoundly changed the morphology of the Aβ42 fibrils. The short Aβ42 fibrils disappeared, and longer fibrils composed of visible subfilaments with occasional twists were observed (Fig. 2*D*), but no regular periodicity could be discerned.

As described above, the polymerized Aβ peptide preparations were resistant to limited PK digestion, which also did not alter the ultrastructure of Aβ40 or Aβ42 polymers as shown by TEM (Fig. S2). This finding is consistent with our earlier study reporting that the morphology of the fibrils purified from the brains of Tg (APP23) mice was unaltered by limited proteolysis (11).

To measure the Aβ prion infectivity of Aβ40 and Aβ42 preparations, we intracerebrally inoculated aliquots into 6-wk-old Tg(APP23:*Gfap*-luc) mice and measured the BLI signal at 14-d intervals. At ∼150 dpi, the BLI signal in the brains of mice injected with Aβ40 or Aβ42 began to exhibit a sustained increase, whereas the bioluminescence in uninoculated mice remained unchanged (Fig. 3 *A* and *B*). The increase in the BLI signal reflects the elevated expression of the luciferase transgene, which is driven by the *Gfap* promoter and therefore reflects the up-regulation of the *Gfap* gene induced by Aβ deposition (10).

At 330 dpi, the bigenic mice were killed, and their brains were removed for biochemical and histopathological studies. Levels of PK-resistant Aβ were markedly increased in the brains of inoculated bigenic mice compared to uninoculated controls (Fig. 3 *C*–*F*). The brain levels of protease-resistant Aβ were similar whether the inoculated mice received Aβ40 or Aβ42 prions; moreover, polymerization of Aβ in the presence of 0.1% SDS did not alter the brain levels of protease-resistant Aβ.

We measured by ELISA the relative accumulation of Aβ40 and Aβ42 peptides in the brains of the inoculated mice (Fig. S3). As shown, the levels of both Aβ40 and Aβ42 increased 5- to 10-fold after inoculation with either Aβ40 or Aβ42 formed in the absence of SDS (Fig. S3*A*). Similar results were seen with Aβ40 and Aβ42 prions formed in the presence of SDS (Fig. S3*B*).

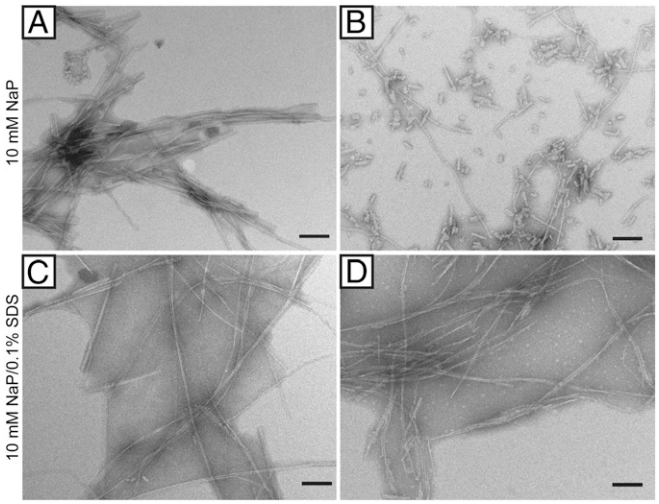

Fig. 2. Electron micrographs of synthetic Aβ40 (*A* and *C*) and Aβ42 (*B* and *D*) prions. In the absence of SDS, both short and long fibrils were found in Aβ40 preparations (*A*) but mostly short fibrils were observed in Aβ42 samples (*B*). Addition of 3.47 mM SDS to the conversion reaction resulted in long fibrillar aggregates, creating similar structures from Aβ40 (*C*) and Aβ42 (*D*). (Scale bars, 100 nm.)

Downloaded at Palestinian Territory, occupied on December 16, 2021
www.manaraa.com

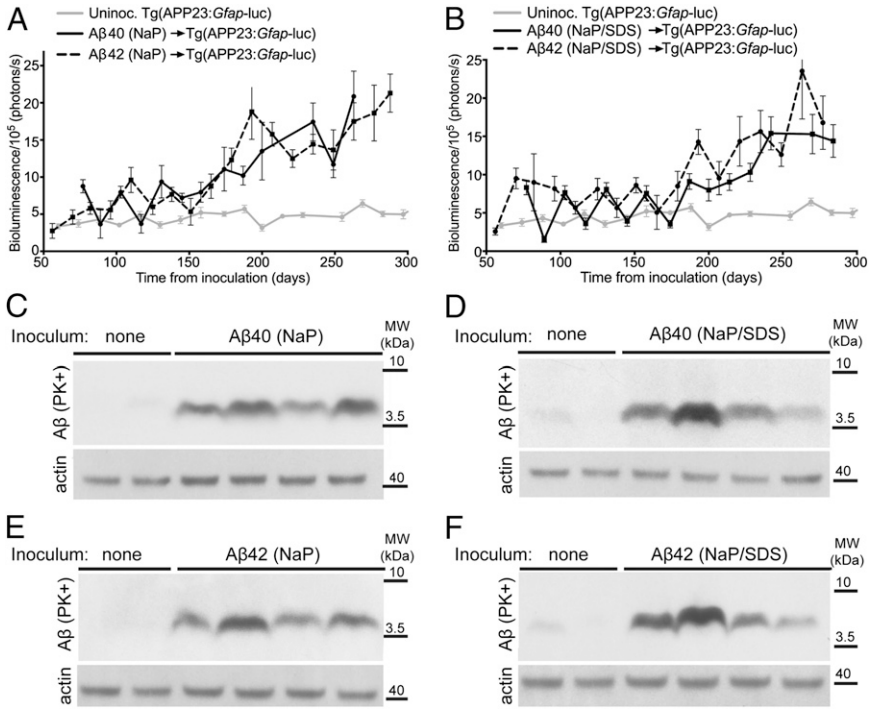

Fig. 3. Inoculation of Tg(APP23:*Gfap*-luc) mice with synthetic Aβ40 and Aβ42 prions. (*A* and *B*) An up-regulation of the BLI signal was observed for all mice injected with synthetic Aβ40 (solid black curves) or synthetic Aβ42 (dashed curves) prepared in NaP (*A*) or NaP/SDS (*B*). Uninoculated mice are shown as a control (gray curves). (*C–F*) PK-resistant Aβ accumulated in the brains of mice injected with synthetic Aβ40 (*C* and *D*) or Aβ42 (*E* and *F*) prepared in NaP (*C* and *E*) or NaP/SDS (*D* and *F*). Total Aβ was probed with antibody 6E10. Actin is shown as a loading control. Molecular weight markers of migrated protein standards are shown in kilodaltons.

To assess the regional deposition of Aβ, fixed sections were immunostained with 4G8 anti-Aβ mAb (Covance). All of the inoculated mice exhibited Aβ plaques distributed along the corpus callosum proximal to the CA1 region of the hippocampus (Fig. S3 *C–F*), which appears to be an inoculation-dependent phenotype for prion transmission in rodents. This pathologic signature of prion transmission to rodents was first recognized in mice inoculated with scrapie prions composed of the prion protein (PrP) (13) and more recently with the transmission of Aβ prions (6, 10, 11). Adjacent sections were stained with Thioflavin S (ThioS) or H&E to assess amyloid deposition and brain histopathology, respectively (Fig. S4). The Aβ plaques stained intensely with ThioS, demonstrating the accumulation of Aβ amyloid fibrils, which was ndependent of the Aβ isoform used for inoculation. Aβ42-inoculated Tg(APP23) mice killed at 30 dpi did not show any residual inoculum (Fig. S5), demonstrating that the pathology observed at 330 dpi was due to nascent Aβ prion deposition.

Next, we measured the number and size of plaques in the brains of mice inoculated with Aβ40 or Aβ42 and killed at 330 dpi. Brain sections were stained with ThioS to determine the number of amyloid plaques and immunostained for GFAP as a marker for reactive astrocytes. Mice injected with synthetic Aβ42 prions formed with NaP alone contained significantly more individual plaques (Fig. 4 and Fig. S6) than those receiving Aβ40 prions formed under the same condition (Fig. 4 and Fig. S6). The greater plaque number was accompanied by a reduction in plaque size (Fig. 4), which was consistent with the overall amount of accumulated Aβ being similar for the two experiments (Fig. S3 *A* and *B*). The greater number of plaques was also accompanied by a more intense astrocytic gliosis (Fig. 4), which may be a consequence of plaque number and composition. When synthetic Aβ prions prepared with 0.1% SDS were injected, the difference in the number of amyloid plaques and the severity of astrocytic gliosis induced by Aβ42 prions were no longer evident (Fig. 4 and Fig. S6).

Having found elevated brain levels of Aβ40 and Aβ42 (Fig. S3 *A* and *B*) and that different synthetic Aβ prions produce distinct size distributions of ThioS-positive plaques (Fig. 4), we speculated that these differences are caused by the molecular composition of individual plaques. To investigate this possibility, we analyzed the deposits by double immunofluorescent labeling with antibodies

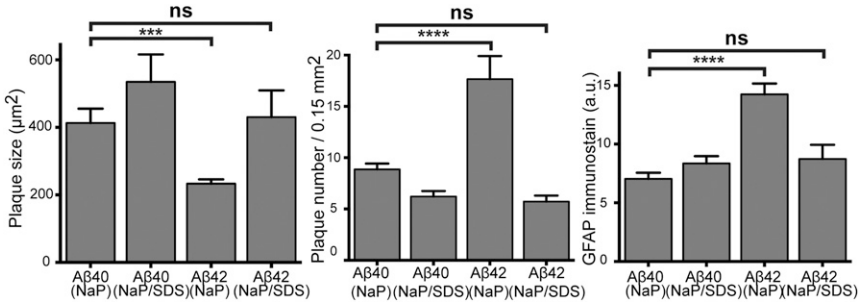

Fig. 4. Reactive astrogliosis associated with the induced deposition patterns of synthetic Aβ prions. Quantification of ThioS-positive plaques in the corpus callosum and dorsal CA1 hippocampal field. The size (*Left*) and number (*Center*) of induced amyloid plaques were significantly different following inoculation with synthetic Aβ42 and Aβ40 prions formed with NaP alone; these differences were not observed for the Aβ peptides polymerized in the presence of SDS. The greater number of plaques in animals inoculated with synthetic Aβ42(NaP) prions was accompanied by significantly increased reactive astrogliosis (*Right*). Data shown as mean ± SEM acquired from three to five animals per experimental group (***$P < 0.001$, ****$P < 0.0001$; ns, not significant).

NEUROSCIENCE
Downloaded at Palestinian Territory, occupied on December 16, 2021
www.manaraa.com

specific to Aβ40 and Aβ42 using confocal fluorescence microscopy. Despite similarities in total Aβ levels in bigenic mice inoculated with either Aβ40 or Aβ42, the patterns of Aβ deposition were dramatically different when compared and quantified using Aβ40- and Aβ42-specific mAbs. Following inoculation of Aβ40 prions prepared in the absence of SDS, bigenic mice showed plaques along the corpus callosum proximal to the CA1 region of the hippocampus; these plaques were composed of more Aβ40 than Aβ42 (Fig. 5*A* and Fig. S7*A*). In contrast, bigenic mice inoculated with Aβ42 prions (prepared in the absence of SDS) produced more plaques that were widely scattered along the corpus callosum; these plaques were composed predominantly of Aβ42 (Fig. 5*B* and Fig. S7*B*). The differences in plaque composition, distribution, and abundance were abolished when the synthetic Aβ prions were prepared in the presence of 0.1% SDS. The plaques contained similar amounts of Aβ40 and Aβ42, and they were tightly distributed along the corpus callosum (Fig. 5 *C* and *D* and Fig. S7 *C* and *D*). Age-matched controls showed very few plaques (Fig. 5*E* and Fig. S7*E*), but as expected, an uninoculated 2-y-old, control bigenic mouse showed widely distributed plaques (Fig. 5*F* and Fig. S7*F*). These different pathogenic signatures demonstrated that inoculation of a particular Aβ prion preparation does not simply accelerate the spontaneous phenotype found in old Tg(APP23) mice, but it also dictates the histopathological phenotype.

Although the plaques that accompanied infection with Aβ40 and Aβ42 prions prepared without SDS were compact, those induced by Aβ prions prepared in the presence of SDS were more diffuse (Fig. 6, cf. *A* and *B* to *C* and *D*). To quantify the differences in plaque composition, we compiled high-resolution, confocal z-stacks of plaques in the corpus callosum and cerebral cortex. Following image acquisition, we analyzed the relative fluorescence levels of Aβ42 and Aβ40 antibody labeling in individual plaques. In control mice that developed spontaneous disease (2 y old), the relative Aβ40/Aβ42 fluorescence ratio in hippocampal plaques was ∼1.5, which did not change on inoculation with Aβ40 prions prepared in the absence of SDS (Fig. 6*G*). In contrast, synthetic Aβ42 prions produced in the absence of SDS induced plaques with significantly higher levels of Aβ42 antibody labeling, reducing the Aβ40/Aβ42 ratio to ∼0.8 ($P < 0.0001$). Following inoculation with either Aβ40 or Aβ42 prepared in the presence of SDS, the resulting Aβ40/Aβ42 ratios were similar, indicating that no isoform-specific differences were induced. Similar findings were obtained in the adjacent cerebral cortex area, demonstrating that isoform-specific self-propagation was not restricted to a single brain region (Fig. 6*H*).

The specificity for isoform-specific seeding was even more pronounced when we quantified small diffuse plaques containing only Aβ42 that had weak to no ThioS labeling (Fig. S8). We evaluated entire brain hemispheres for the occurrence of these plaques and found them to be mostly present in the cortices of mice inoculated with Aβ42(NaP) prions, whereas they were rarely found in age-matched controls or mice inoculated with Aβ40 (NaP), Aβ40(NaP/SDS), or Aβ42(NaP/SDS) prions. Moreover, these diffuse Aβ42 plaques are known to appear spontaneously only in much older animals that exhibit a large amyloid burden, suggesting that synthetic Aβ42(NaP) prions specifically seeded the appearance of these particular plaques (14).

Discussion

In the studies reported here, we described the more efficient production of synthetic Aβ prions using an alternative procedure for the polymerization of Aβ peptides into amyloid fibrils compared with earlier studies (11). Our current preparation method rendered the majority of the Aβ peptides resistant to limited proteolysis and reduced the BLI incubation time by ∼100 d compared with our previous study, in which <10% of the synthetic Aβ peptide was protease resistant (Figs. 1 and 3). Differences in the Aβ40 and Aβ42 prion preparations were reflected in the pathological phenotypes in the brains of Tg(APP23:*Gfap*-luc) mice. Moreover, the properties of the Aβ42 prions that distinguished them from the Aβ40 prions could be abolished by performing the polymerization reaction in the presence of 0.1% SDS.

The synthetic Aβ42 prions were found to be distinct from the Aβ40 prions when prepared in the absence of SDS in several respects. First, the Aβ42 amyloid polymers formed more rapidly than the Aβ40 fibrils, as measured by ThT fluorescence (Fig. 1). Second, Aβ42 fibrils were relatively short but polymerized into much longer structures when prepared in the presence of SDS (Fig. 2). Third, inoculation of synthetic Aβ40 prions induced large amyloid plaques that were composed predominantly of Aβ40 resulting in an Aβ40/Aβ42 ratio of ∼1.5 (Fig. 6). Aβ42 prions produced significantly more but smaller amyloid plaques; these plaques were found in the corpus callosum, hippocampus, and cerebral cortex (Figs. 5 and 6) with an Aβ40/Aβ42 ratio of ∼0.8. Our findings are consistent with surface plasmon resonance measurements showing that homogeneous interactions between these peptides are preferred over heterogeneous interactions (15); a similar phenomenon was found with PrP prions in Tg mice expressing both hamster and mouse PrP (16).

Although Aβ40 and Aβ42 are the two most abundant peptides cleaved from APP by γ-secretase, several other Aβ peptides have also been identified, including Aβ38 and Aβ43. These different-length peptides result from the infidelity of γ-secretase and

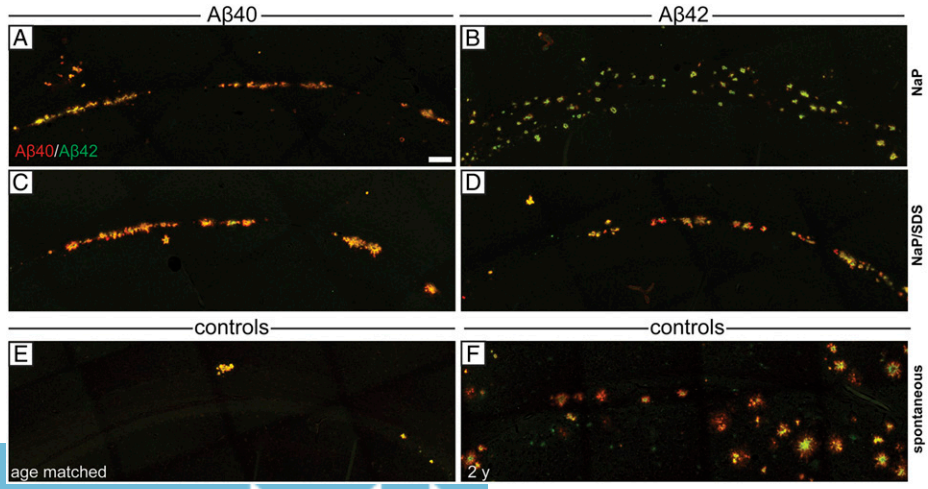

Fig. 5. Composition of Aβ deposition in the brains of Tg(APP23:*Gfap*-luc) mice inoculated with synthetic Aβ40 (*Left*) or Aβ42 (*Right*) prepared in NaP or NaP/SDS. (*A*–*D*) Fixed brain slices from mice at ∼330 dpi were double-immunolabeled for Aβ40 (red) and Aβ42 (green). Different immunolabeling patterns were observed along the corpus callosum following inoculation with Aβ40(NaP) (*A*) and Aβ42(NaP) (*B*). In contrast, following inoculation with Aβ40(NaP/SDS) (*C*) and Aβ42(NaP/SDS) (*D*), no difference in the pattern of amyloid deposition could be detected. Fixed brain slices from uninoculated, age-matched mouse (405 d of age, *E*) and a spontaneously ill, 2-y-old mouse (*F*) are shown as controls. Micrographs were taken with a Leica SP8 confocal microscope. (Scale bar in *A* applies to all panels, 100 μm.)

Downloaded at Palestinian Territory, occupied on December 16, 2021
www.manaraa.com

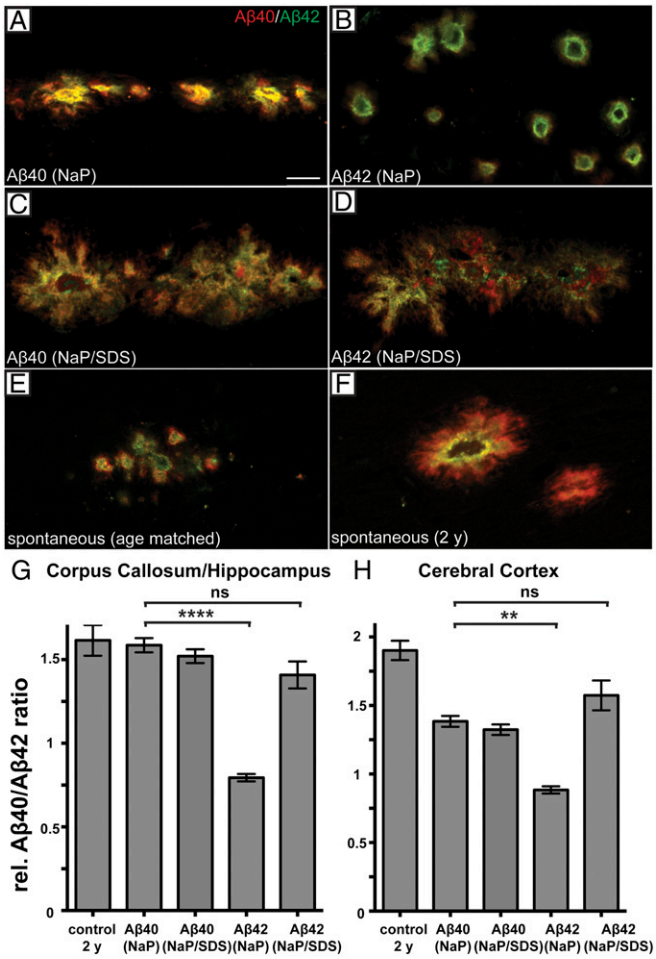

Fig. 6. Synthetic Aβ42 formed under NaP buffer induces a significant increase in Aβ42 levels associated with individual plaques. (*A–F*) Fixed brain slices double-immunolabeled for Aβ40 (red) and Aβ42 (green) were imaged by confocal microscopy (63 × 1.2 NA). Confocal Z-projections of images show plaques in the corpus callosum of mice inoculated with synthetic Aβ40 (*A* and *C*) or Aβ42 (*B* and *D*) formed in NaP (*A* and *B*) or in NaP/SDS (*C* and *D*). Slices were taken from mice killed at 330 d after inoculation. Z-projections from an age-matched mouse (*E*; 405 d of age) and a spontaneously ill, 2-y-old mouse (*F*) are shown for comparison. (Scale bar in *A* applies to *B–F*, 15 μm.) (*G* and *H*) Quantification of the relative Aβ40/Aβ42 fluorescence ratio per individual plaque in confocal Z-projections. Injection with Aβ42(NaP) resulted in a significant increase in Aβ42 deposition in hippocampal (*G*; ****$P < 0.0001$) and cerebral cortex areas (*H*; **$P < 0.01$) compared with mice inoculated with Aβ40(NaP). Data shown as mean ± SEM acquired from three to five animals per experimental group (ns, not significant).

complicate the interpretation of many AD studies, including the data reported here. Our findings with Aβ42 demonstrated that two preparations with and without 0.1% SDS resulted in profoundly different physical and biological properties. These differences argue for the existence of distinct Aβ prion strains.

For many years, the existence of prion strains was used as an argument against the proposal that prions causing scrapie of sheep and CJD could be composed solely of protein (17). A frequent refrain was that the biological variation manifest by different strains of scrapie prions demanded the presence of a nucleic acid. Subsequently, evidence was found for the suggestion that prion strains represent different conformers of PrP^{Sc} (18–21). The discovery of yeast prions accelerated biophysical studies showing that two different [PSI^+] prion stains have distinct structures (22, 23). More recently, it was possible to produce different strains of PrP prions by varying the conditions of polymerization of recombinant mouse PrP(89–230) (24).

The analysis of different prion strains has been facilitated when the amino acid sequence of the precursor protein remains constant. However, in some instances, the human PrP residue 129 and murine PrP positions at 108 and 189 are polymorphic (25–28). The difficulties surrounding studies of Aβ prion strains are highlighted by a study using Tg(APP23) and Tg(APPPS1) mice: the former produce much more Aβ40 than Aβ42, whereas the latter produced the opposite (29). The ratio of Aβ40/Aβ42 was significantly higher when Tg(APP23) mice were inoculated with brain extracts from Tg(APP23) mice than with extracts from Tg (APPPS1) mice. When Tg(APPPS1) mice were inoculated with the two extracts, no significant difference in the Aβ40/Aβ42 ratio was found between the two groups. These findings were interpreted as evidence for the strain-like properties of Aβ prions. In contrast, the studies reported here used synthetic Aβ peptides, and the inocula contained either Aβ40 or Aβ42 but not both.

Although differences in polymerization kinetics persisted after addition of SDS (Fig. 1), the ultrastructure of Aβ42 fibrils became indistinguishable from that of Aβ40 fibrils prepared in the presence or absence of SDS, arguing for a similar quaternary structure (Fig. 2). Consistent with the TEM results, the synthetic Aβ42 prions prepared in the presence of SDS produced Aβ plaques with an Aβ40/Aβ42 ratio of ∼1.5, similar to that found with Aβ40 prions prepared with or without SDS (Figs. 5 and 6).

The conformational manipulation of the PrP protein with SDS was initially used to induce a β sheet-rich state in recombinant and natural occurring PrP (30) and was later used to promote amyloid formation (31, 32). The anionic surface created by SDS has been found to promote fibril formation for a variety of proteins (33). In earlier studies by others, 0.2% SDS was reported to induce globular aggregates of Aβ; moreover, no fibrils were detected by atomic force microscopy (34). Our findings are consistent with those of others, who found that SDS initially induced globular aggregates of Aβ, which later assembled spontaneously into fibrils (35).

From the data presented here, we conclude that two strains of synthetic Aβ42 prions were formed: the first strain was formed in the absence of SDS and the second was formed in the presence of 0.1% SDS. We found that comparing the two Aβ42 prion strains to the Aβ40 prions instructive: first, Aβ40 and Aβ42 prions prepared in the absence of SDS exhibited different physical and biological properties. Second, Aβ40 prions prepared in either the absence or presence of SDS were virtually indistinguishable from Aβ42 prions prepared in the presence of SDS with respect to their physical and biological properties. Structural studies of Aβ peptides from the brains of AD patients (36) provide a possible explanation for the observed differences in morphology between synthetic Aβ40 and Aβ42 prions. Val39 and Val40 are buried near the core, interacting with other hydrophobic residues, leaving only a small space to accommodate the additional two C-terminal residues of Aβ42. It will be interesting to determine whether Aβ40 and Aβ42 (with and without SDS) are conformationally homogeneous or represent a mixture of conformational isoforms.

As noted above, the production of both Aβ40 and Aβ42 in the brains of mice may preclude us from passaging our synthetic strains in an environment where we can test if they breed true; nevertheless, such studies are in progress. When we compared WT Aβ prions to those from a patient who died of fAD caused by the Arctic mutation E22G, we found that this substitution reduced the conformational stability of the protease-resistant Aβ and significantly increased the perivascular deposition of Aβ38 in the brains of Tg (APP23:*Gfap*-luc) mice (37). Moreover, this pathology persisted on serial passage in these bigenic mice that produce only WT Aβ.

In AD, the pathogenesis is likely to be more complex than can be modeled in rodents considering the much larger number of neurons in the human brain, increased diversity of neural cell types, and the much longer time frame for the disease to manifest.

NEUROSCIENCE

Downloaded at Palestinian Territory, occupied on December 16, 2021
www.manaraa.com

Furthermore, when brain samples from AD patients were analyzed for Aβ peptides, a plethora of distinct Aβ isoforms was found (38). Our findings with Aβ40 and Aβ42 prions raise the possibility that all Aβ isoforms may adopt distinct conformations, each of which undergoes self-propagation. This molecular mixture of Aβ prion strains may be partially responsible for the variations in clinical and pathological presentations observed in patients with AD. An example for this phenomenon was recently demonstrated in patients with fAD mutations within the Aβ sequence (amino acids 1–42): some mutations within the Aβ sequence seemed to stimulate the incorporation of Aβ38 into plaques and perivascular areas (39).

It seems likely that deciphering and cataloging strains of Aβ prions in the brains of AD patients will prove critical in developing accurate and informative molecular diagnostics, which may be just as important in creating therapeutics. Studies of anti-PrP prion drugs have demonstrated the development of drug-resistant and -dependent strains of prions (40–42). Moreover, we found that distinct PrP prion strains responded differently to drugs that prolonged the lives of mice (41). The insights gained from studies of synthetic Aβ prions should aid in deciphering the molecular pathogenesis of AD, for which there is not any medicine that halts or even slows this dementing illness.

Material and Methods

Preparation of Synthetic Aβ Aggregates. The WT Aβ40/42 peptide was purchased from Bachem. Lyophilized peptides were dissolved to 5 mg/mL in hexafluoroisopropanol (HFIP) and separated in 200-μg aliquots. HFIP was evaporated in a speedvac and stored at −20 °C. For conversion, the dried peptide film was solubilized in 20 μL DMSO and diluted with 980 μL of aqueous buffer solutions containing 10 mM NaP with or without 3.47 mM SDS. Samples were incubated at 37 °C for 72 h in 1.5-mL centrifugation tubes under constant agitation at 900 rpm. The resulting samples were spun down for 1 h at 100,000 × *g*, and the pellet was resuspended in 100 μL PBS at 2 mg/mL. Samples were further analyzed or diluted, snap-frozen in liquid nitrogen, and stored at −80 °C before inoculation.

PK Digestion of Synthetic and Brain-Derived Aβ Aggregates. After incubation for 72 h at 37 °C, synthetic Aβ samples in PBS were adjusted to 0.2 mg/mL with PBS, and PK (Thermo Scientific) was added to a final concentration of 50 μg/mL. After digestion for 1 h at 37 °C under constant agitation, the reaction was stopped by the addition of 1 mM PMSF. NuPAGE sample buffer (4×; Invitrogen) was added to a final concentration of 1× before SDS/PAGE. For digestion of brain-derived aggregates, 500 μg of total protein was prepared in 500 μL of lysis buffer (PBS, 0.5% deoxycholate, 0.5% Nonidet P-40) containing 20 μg/mL PK (PK:protein ratio of 1:50). Digestions were performed at 37 °C for 1 h under constant agitation and then stopped by the addition of 1 mM PMSF. Samples were ultracentrifuged for 1 h at 100,000 × *g*, and the resulting pellet was resuspended in 50 μL of 1× NuPAGE sample buffer.

ACKNOWLEDGMENTS. We thank the staff at the Hunter's Point animal facility for assistance with the animal experiments and Marta Gavidia for mouse genotyping. The Tg(*Gfap*-luc) mice were a generous gift from Caliper Life Sciences. This work was supported by National Institutes of Health Grants AG002132, AG010770, AG021601, AG031220, and NS041997 and gifts from the Sherman Fairchild Foundation and Rainwater Charitable Foundation. J.S. was supported by a fellowship from the Glenn Foundation for Medical Research and J.C.W. was supported by a K99 grant from the National Institute on Aging (AG042453).

1. Schellenberg GD, Montine TJ (2012) The genetics and neuropathology of Alzheimer's disease. *Acta Neuropathol* 124(3):305–323.
2. Prusiner SB (2012) Cell biology. A unifying role for prions in neurodegenerative diseases. *Science* 336(6088):1511–1513.
3. Rademakers R, Neumann M, Mackenzie IR (2012) Advances in understanding the molecular basis of frontotemporal dementia. *Nat Rev Neurol* 8(8):423–434.
4. Goudsmit J, et al. (1980) Evidence for and against the transmissibility of Alzheimer disease. *Neurology* 30(9):945–950.
5. Ridley RM, Baker HF, Windle CP, Cummings RM (2006) Very long term studies of the seeding of beta-amyloidosis in primates. *J Neural Transm* 113(9):1243–1251.
6. Meyer-Luehmann M, et al. (2006) Exogenous induction of cerebral beta-amyloidogenesis is governed by agent and host. *Science* 313(5794):1781–1784.
7. Mullan M, et al. (1992) A pathogenic mutation for probable Alzheimer's disease in the APP gene at the N-terminus of beta-amyloid. *Nat Genet* 1(5):345–347.
8. Sturchler-Pierrat C, et al. (1997) Two amyloid precursor protein transgenic mouse models with Alzheimer disease-like pathology. *Proc Natl Acad Sci USA* 94(24):13287–13292.
9. Eisele YS, et al. (2010) Peripherally applied Abeta-containing inoculates induce cerebral beta-amyloidosis. *Science* 330(6006):980–982.
10. Watts JC, et al. (2011) Bioluminescence imaging of Abeta deposition in bigenic mouse models of Alzheimer's disease. *Proc Natl Acad Sci USA* 108(6):2528–2533.
11. Stöhr J, et al. (2012) Purified and synthetic Alzheimer's amyloid beta (Aβ) prions. *Proc Natl Acad Sci USA* 109(27):11025–11030.
12. Stine WB, Jungbauer L, Yu C, LaDu MJ (2011) Preparing synthetic Aβ in different aggregation states. *Methods Mol Biol* 670:13–32.
13. Scott M, et al. (1989) Transgenic mice expressing hamster prion protein produce species-specific scrapie infectivity and amyloid plaques. *Cell* 59(5):847–857.
14. Sturchler-Pierrat C, Staufenbiel M (2000) Pathogenic mechanisms of Alzheimer's disease analyzed in the APP23 transgenic mouse model. *Ann N Y Acad Sci* 920:134–139.
15. Pauwels K, et al. (2012) Structural basis for increased toxicity of pathological $a\beta_{42}$:$a\beta_{40}$ ratios in Alzheimer disease. *J Biol Chem* 287(8):5650–5660.
16. Prusiner SB, et al. (1990) Transgenetic studies implicate interactions between homologous PrP isoforms in scrapie prion replication. *Cell* 63(4):673–686.
17. Bruce ME (1993) Scrapie strain variation and mutation. *Br Med Bull* 49(4):822–838.
18. Prusiner SB (1991) Molecular biology of prion diseases. *Science* 252(5012):1515–1522.
19. Bessen RA, Marsh RF (1994) Distinct PrP properties suggest the molecular basis of strain variation in transmissible mink encephalopathy. *J Virol* 68(12):7859–7868.
20. Telling GC, et al. (1996) Evidence for the conformation of the pathologic isoform of the prion protein enciphering and propagating prion diversity. *Science* 274(5295): 2079–2082.
21. Ayers JI, et al. (2011) The strain-encoded relationship between PrP replication, stability and processing in neurons is predictive of the incubation period of disease. *PLoS Pathog* 7(3):e1001317.
22. Wickner RB (1994) [URE3] as an altered URE2 protein: Evidence for a prion analog in *Saccharomyces cerevisiae*. *Science* 264(5158):566–569.
23. Tanaka M, Collins SR, Toyama BH, Weissman JS (2006) The physical basis of how prion conformations determine strain phenotypes. *Nature* 442(7102):585–589.
24. Colby DW, et al. (2009) Design and construction of diverse mammalian prion strains. *Proc Natl Acad Sci USA* 106(48):20417–20422.
25. Owen F, Poulter M, Collinge J, Crow TJ (1990) Codon 129 changes in the prion protein gene in Caucasians. *Am J Hum Genet* 46(6):1215–1216.
26. Parchi P, et al. (2010) Agent strain variation in human prion disease: Insights from a molecular and pathological review of the National Institutes of Health series of experimentally transmitted disease. *Brain* 133(10):3030–3042.
27. Carlson GA, et al. (1986) Linkage of prion protein and scrapie incubation time genes. *Cell* 46(4):503–511.
28. Westaway D, et al. (1987) Distinct prion proteins in short and long scrapie incubation period mice. *Cell* 51(4):651–662.
29. Heilbronner G, et al. (2013) Seeded strain-like transmission of β-amyloid morphotypes in APP transgenic mice. *EMBO Rep* 14(11):1017–1022.
30. Jansen K, et al. (2001) Structural intermediates in the putative pathway from the cellular prion protein to the pathogenic form. *Biol Chem* 382(4):683–691.
31. Xiong L-W, Raymond LD, Hayes SF, Raymond GJ, Caughey B (2001) Conformational change, aggregation and fibril formation induced by detergent treatments of cellular prion protein. *J Neurochem* 79(3):669–678.
32. Stöhr J, et al. (2008) Mechanisms of prion protein assembly into amyloid. *Proc Natl Acad Sci USA* 105(7):2409–2414.
33. Rangachari V, et al. (2007) Amyloid-β(1-42) rapidly forms protofibrils and oligomers by distinct pathways in low concentrations of sodium dodecylsulfate. *Biochemistry* 46(43):12451–12462.
34. Barghorn S, et al. (2005) Globular amyloid β-peptide oligomer - a homogenous and stable neuropathological protein in Alzheimer's disease. *J Neurochem* 95(3):834–847.
35. Abelein A, et al. (2013) Formation of dynamic soluble surfactant-induced amyloid β peptide aggregation intermediates. *J Biol Chem* 288(32):23518–23528.
36. Lu JX, et al. (2013) Molecular structure of β-amyloid fibrils in Alzheimer's disease brain tissue. *Cell* 154(6):1257–1268.
37. Watts JC, et al. (2014) Serial propagation of distinct strains of Aβ prions from Alzheimer's disease patients. *Proc Natl Acad Sci USA* 111:10323–10328.
38. Portelius E, et al. (2010) Mass spectrometric characterization of brain amyloid beta isoform signatures in familial and sporadic Alzheimer's disease. *Acta Neuropathol* 120(2):185–193.
39. Moro ML, et al. (2012) *APP* mutations in the Aβ coding region are associated with abundant cerebral deposition of Aβ38. *Acta Neuropathol* 124(6):809–821.
40. Ghaemmaghami S, et al. (2009) Continuous quinacrine treatment results in the formation of drug-resistant prions. *PLoS Pathog* 5(11):e1000673.
41. Berry DB, et al. (2013) Drug resistance confounding prion therapeutics. *Proc Natl Acad Sci USA* 110(44):E4160–E4169.
42. Oelschlegel AM, Weissmann C (2013) Acquisition of drug resistance and dependence by prions. *PLoS Pathog* 9(2):e1003158.

Downloaded at Palestinian Territory, occupied on December 16, 2021

www.manaraa.com